Fluid Phase Equilibria 594 (2025) 114344

Contents lists available at ScienceDirect

Fluid Phase Equilibria

journal homepage: www.journals.elsevier.com/fluid-phase-equilibria

A robust setup for efficient characterization of multicomponent vapor-liquid equilibria using Raman spectroscopy

Marvin Kasterke, Leo Bahr, Hans-Jürgen Koß, Thorsten Brands *

Institute of Technical Thermodynamics, RWTH Aachen University, Schinkelstraße 8, 52062 Aachen, Germany

ARTICLE INFO

Keywords:
Vapor-liquid equilibirum
Raman spectroscopy
Isothermal
Static-analytic
In-situ

ABSTRACT

Vapor-liquid equilibrium (VLE), a crucial thermodynamic property in diverse industrial processes, assumes paramount significance in the development, optimization, and operation of separation processes and various applications. Despite their central role, large sample volumes, long measurement times and the handling of the apparatus are a challenge for the precise determination of VLE data. In response to these challenges, we present an innovative Raman spectroscopy-based measurement setup that enables fast, accurate and user-friendly characterization of VLE. The application of Raman spectroscopy enables non-invasive analysis of vapor and liquid-phases in small sample volumes (<3 ml) for multiple VLE data points. The usage of a compact isothermal VLE measurement cell ensures rapid and reliable VLE control. The combination of the equilibrium cell with a highly confocal fiber-coupled Raman probe in backscattering configuration and a high-throughput spectrometer establishes an efficient setup for quantifying VLE data in a broad range of conditions. The setup has been validated for vapor pressure curves of methyl tert-butyl ether (MTBE), isooctane (2,2,4-trimethylpentane) and cyclohexane for a temperature range of 283.15 K to 333.15 K and the measurement of the binary VLE MTBE-isooctane at 318 .15K. the setup allows a highly efficient access to VLE data of industrial relevance.

1. Introduction

Vapor Liquid Equilibrium (VLE) data are at the core of the chemical industry [1]. In chemical engineering and other related disciplines, they represent a cornerstone for reliable and optimal process design, e.g. for thermal separation [2,3]. These process steps often decide on the feasibility of whole production processes from both engineering and economic standpoints. As ecological aspects rapidly gain in importance, optimizing the highly energy-demanding thermal separation processes is a game-changing factor. As they account for 10–15 % of today's total world energy demand [4,5], even small reductions have significant environmental benefits.

To obtain VLE data, chemical engineers have three options: database lookup, predictive thermophysical property methods, or experimental measurement. Commonly, the costs and procurement time of these options rise in the same order.

Experimentally acquired tabulated VLE data, e.g. from the National Institute of Standards and Technology (NIST) or the Dortmund Database (DDB), can often be scarce. Even for well-known mixtures of industrial significance, only a few data points at certain temperatures and pressures exist [1]. For many "new", promising substances there is no data available at all.

Simulation tools are constantly drawing more attention as computational power availability rises and costs decrease. Equation of state (EOS) methods such as the well-established PSRK (Predictive Soave-Redlich-Kwong) [6] or the more recent PC-SAFT (statistical associating fluid theory) [7] have proven to be valuable tools for chemical engineers. Besides these EOS, activity coefficient models such as UNIFAC (Universal Quasichemical) [8] or quantum-based solvation models (COSMO-RS) [9] deliver highly accurate predictions on thermophysical properties (such as VLE) for well-known substances. For relatively unknown substances, however, predictions are challenging and often inaccurate especially if experimental data on basic thermodynamic parameters (e.g. pure-component vapor pressures) is still missing. At this point, the question arises whether the calculated values can be trusted without experimental validation.

At first sight, both favorable options database lookup and simulation rely on experimental measurements, especially for multi-component (ternary and above) VLE data of previously less investigated substances. In general, highly accurate VLE data, essential for efficient

* Corresponding author.
E-mail addresses: marvin.kasterke@ltt.rwth-aachen.de (M. Kasterke), thorsten.brands@ltt.rwth-aachen.de (T. Brands).

https://doi.org/10.1016/j.fluid.2025.114344
Received 29 November 2024; Received in revised form 4 January 2025; Accepted 18 January 2025
Available online 19 January 2025

process design, is still only achievable by direct experimental methods. However, the measurement of VLE data for mixtures with common methods is expensive [1,10,11]. This defines the starting point for the development of new, efficient ways to characterize VLE experimentally.

2. State of the art: experimental VLE determination

Experimental procedures for VLE data determination are divided into two classes: synthetic and analytical methods. A comprehensive overview is presented in [12]. In synthetic methods, mixtures with known compositions are synthesized. After equilibration, without further analysis of the phases, the temperature or pressure of the system is altered until variations of physical or thermodynamic properties are observed. For example, a phase transition can be visually detected by varying either temperature or pressure, with pressure changes being the more commonly used approach. For binary systems, VLE data can often be obtained directly from the observed phase change without requiring computational models or mass balances, as their phase behavior is relatively straightforward. In contrast, for multicomponent systems, the complexity of interactions necessitates the use of mass balances and models to accurately determine phase boundaries and compositions [12–14].

Thus, synthetic methods are experimentally simple, fast, and cost-effective, making them a common choice [9,10]. However, they exhibit several unique drawbacks, particularly due to their reliance on computational models to interpret experimental data. In contrast, methods that directly measure phase compositions are less susceptible to these model-driven errors. A fundamental limitation of synthetic methods is that they can only provide one data point on the phase boundary per experiment, which significantly increases the number of experiments required to map the entire phase diagram, especially for multicomponent systems. Additionally, synthetic methods often necessitate the precise preparation of initial mixtures, and any errors in this process directly affect the results. Unlike analytical techniques, which can directly measure the composition of both the vapor and liquid-phases, synthetic methods must rely on computational models to derive VLE data, making them particularly vulnerable to inaccuracies when handling complex systems.

In contrast, analytical methods focus on the direct quantification of the composition of the vapor and liquid-phases in equilibrium and, hence, are less susceptible to these model-driven errors. By analyzing both phases, these methods provide the trajectory of the phase envelopes (saturation lines) in each experiment, independent of the analytical technique employed or the number of components involved. The exact knowledge of the initial compositions is not required. Conventionally, phase compositions are measured via sampling in combination with *ex-situ* analytical techniques (e.g., gas chromatography). Dynamic devices in which the fluids circulate through the equilibrium apparatus under a constant pressure allow for easy sample access [15]. However, the circulation leads to gradients in temperature and concentration and, hence, a disturbance of the equilibrium. Static devices avoid this drawback and, thus, yield “the truest equilibrium” [15]. Most static devices consist of enclosed equilibrium cells containing the mixture at equilibrium at a defined temperature [10].

In general, for both dynamic and static devices, sampling represents a well-known error source because it is invasive, i.e., it can disturb the equilibria and cause loss of components [16]. Its negative influences can be weakened by minimizing the relative sampling volume, either by enlarging the substance volumes in the apparatus or by reducing the absolute sample volume. The latter is restricted by the analytical devices. Large apparatus volumes are critical cost and time factors due to the required amount of substance and long equilibration times. Especially for multi-component mixtures, the necessary amount of substance heavily increases. This causes problems particularly for the evaluation of novel substances in early innovation stages because these substances often cannot be synthesized quickly and economically in the required large amounts.

As shown, avoiding sampling offers many benefits. The 2020 special issue of ACS *Journal of Chemical & Engineering Data* [17] highlights some of these innovative techniques such as Raman spectroscopy [18], ultrasound [19], and nuclear magnetic resonance [20]. Other methods include differential scanning calorimetry (DSC) [21] that, however, is limited to binary systems.

Raman spectroscopy was already applied various times to analyze VLE, starting in the early 1990s [22]. Due to the low intensities of the Raman signal and limited signal detection capabilities available at the time, recording a single vapor-phase spectrum required extended acquisition times and only worked in combination with photomultiplier and other amplification instrumentation [22]. Vapor-phase characterization remains challenging to this day, particularly at low pressures where the molecular density, and consequently the Raman signal, is minimal. Further studies focused on high-pressure VLE [23,24]. Furthermore, promising progress was achieved by combining Raman spectroscopy and microfluidics [18,25–27], where VLE are formed as a moving plug-flow inside a glass capillary (on a μm scale). The small dimensions are beneficial in terms of sample consumption, pressure stability, and equilibration times. However, challenges arise from a liquid wall film surrounding the vapor-phase as the Raman signal from the vapor-phase is superimposed by the strong liquid-phase signal leading to cross-sensitivities and systematical errors. Its material-dependent mathematic correction limits the generalizability of the method.

Using these techniques in combination with small static cells offers manifold opportunities for efficient and accurate VLE characterization without disturbing the equilibrium. Liebergesell et al. developed the so-called “RAMSPEQU” setup, capable of quantifying high quality VLE data in a highly efficient manner [28]. In addition to providing binary VLE data, Liebergesell et al. demonstrated the possibility of determining a quaternary VLE by measuring the liquid-phase mole fractions and calculating the vapor-phase mole fractions using PCP-SAFT equation of state [29]. Nevertheless, the operation of Liebergesells et al. setup was challenging due to leakage and an error-prone complex optical setup. The operation of the “RAMSPEQU” setup required a completely darkened optical laboratory to eliminate the influence of ambient light. Optics specialists were necessary for maintenance and alignment of the beam path of the “RAMSPEQU” setup. These limitations hindered the broader application of the system. To tackle the issue of useability we present an easy-to-use and overall robust setup to measure high-quality VLE data, even for non-specialists. The novel setup is demonstrated for vapor pressure curves of methyl tert-butyl ether (MTBE), isooctane (2,2,4-trimethylpentane) and cyclohexane and the measurement of the binary VLE MTBE-isooctane at 318.15K.

3. Material and methods: experimental VLE determination

The new experimental setup for VLE measurements is designed with a modular architecture, allowing for maximum flexibility, robustness, and ease of use. The system is divided into three distinct modules: a compact equilibrium cell, a robust, and highly flexible fiber-coupled measurement system as well as a surrounding housing to encapsulate the setup from the environment. The modular design enables different experimental configurations without significant reconfiguration of the entire setup. The compact measurement cell is designed for stability and durability. It features a reliable reach and hold of the equilibrium, integrating seamlessly with tempering systems, which are comprehensively described in 3.1. The compact and robust optical measurement system ensures consistent performance and minimizes maintenance efforts. Fiber-coupling provides a high degree of flexibility. A detailed description can be found in Section 3.2. The housing encapsulates the setup from the environment in terms of excess light, dust and, for calibration processes, even ambient air. For vapor-phase calibration, the Raman signal of the sample needs to be calibrated against nitrogen as

shown in 4.1. Hence, the beam path to be free of nitrogen. Therefore, the housing, where the setup sits in, can be flushed with a noble gas to avoid interference with the nitrogen from ambient air.

3.1. Equilibrium cell and sample handling

At the core of the equilibrium cell setup sits a stainless-steel sample chamber (Fig. 1d)) with a capacity of up to 3 mL. To enable Raman measurements there is an optical access on the top of the sample chamber for vertical optical access. The sample chamber is surrounded by an approx. one Liter tempering bath (Fig 1d)). The temperature control of the setup is maintained by a Haake Phoenix II P50C thermostat (Fig. 1e)), which circulates tempering fluid through the bath surrounding the equilibrium cell. This system ensures stable isothermal conditions during both the equilibration process and the VLE measurements. To prevent condensation on the optical access, a window heating system is employed. A sapphire glass window (25.4 mm Dia., 5 mm Thick, VIS-NIR AR Coated Sapphire Window, Edmund optics) is mounted in an aluminum tube (50 mm outer diameter, 40 mm length) that is temperature-controlled using two 40 Watt heating cartridges (24 V Heating Cartridge 3DF-020, 3D Freunde). The heating cartridges are regulated by a PID controller (Quantrol 100, Jumo), which receives input from a Pt100 sensor at the base of the aluminum tube. This configuration ensures a controlled temperature gradient from the top, where the heating cartridges are located, to the bottom near the sapphire window, keeping the window slightly warmer than its surroundings to prevent condensation and guarantee clear optical access. The connection between the aluminum tube and the stainless-steel sample chamber is sealed using a Polytetrafluoroethylene (PTFE) gasket. The setup is designed to acquire measurements from two distinct positions within the equilibrium cell (vapor-phase and liquid-phase). The different positions are accessed by translating a Raman probe (Fig. 1c)), as described in Section 4.4, using translation stages. An insert is positioned between the tube and the sapphire glass window, designed to block the laser beam (behind the Raman measuring point) during vapor-phase characterization (see Fig. 2). Thus, the insert acts as a beam dump to prevent excitation of liquid-phase Raman signal that can superimpose

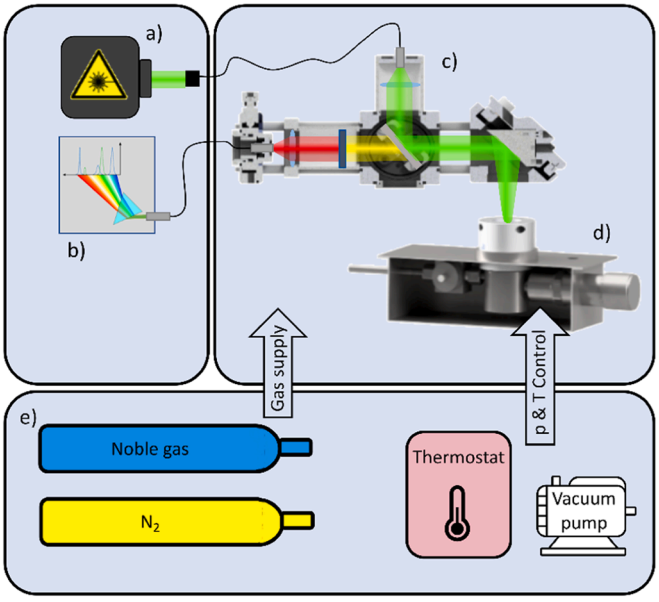

Fig. 1. Measurement setup including benchtop devices a) 532 nm Nd-YAG laser (Genesis CX532–2000 SLM, Coherent), b) high throughput Spectrometer (Raman 532 EXR, Wasatch Photonics), c) highly flexible Raman Probe, d) RaceVLE equilibrium cell and e) conditioning unit with thermostat (Haake Phoenix II P50C thermostat), vacuum pump and gas supply for noble gas flush and nitrogen for calibration purpose.

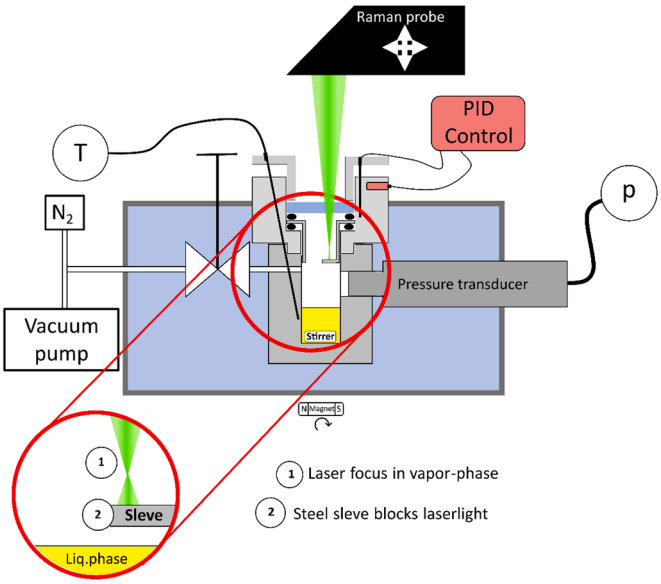

Fig. 2. Conceptional drawing of the RaceVLE equilibrium cell: Traversable Raman probe, sample chamber surrounded by a temperature bath and connected to a nitrogen supply and vacuum pump. Optical access temperature controlled by window heating system. The detail on the left shows the stainless-steel insert and laser focus in the measuring position for the vapor-phase.

the weak vapor-phase signal. The insert is shaped as a sleeve with half of its base removed, allowing selective access to either the liquid or vapor-phase by adjusting the horizontal position of the Raman probe. This dual-phase capability allows for precise Raman measurements across the liquid and vapor-phases of the equilibrium system.

To ensure a reliable seal against the external environment, perfluoroelastomer (FFKM) O-rings are used at both the interface between the tube and the insert, as well as between the insert and the sapphire glass window. The equilibrium cell is equipped with a diaphragm valve (SS-DLS6 MM, Swagelok) for gas handling, which connects the system to both a vacuum pump and a gas supply. The valve and attached piping (6 mm outer diameter, 1 mm wall thickness) are immersed in the tempering bath to maintain isothermal conditions during gas handling operations. This configuration allows for efficient degassing of the system by removing unwanted gases. Furthermore, it provides precise pressure regulation, either by relieving pressure or by introducing gas as needed to maintain the desired experimental conditions, i.e. the indirect calibration as described in Section 4.2. To enhance mass transfer and the equilibration process, the sample chamber incorporates a magnetic PTFE stirrer (flea), which is actuated by a rotating magnet located beneath the tempering bath. This magnet is driven by a NEMA 17 stepper motor controlled by an Arduino Mega 2560, enabling precise and consistent mixing of the sample.

Samples are introduced into the equilibrium cell manually by removing the sapphire window, allowing for easy access for liquid replacement. To ensure accurate temperature determination, a Pt100 sensor (Class A) is embedded in the stainless-steel wall of the equilibrium cell, preventing condensation-related errors on the sensor's surface. Pressure is measured using a pressure transducer (P-31, 0–400 kPa abs., with 0.05 % full-scale uncertainty, WIKA), which is immersed in the tempering bath to ensure stable isothermal conditions. Both pressure and temperature data are recorded at one-second intervals during equilibration and VLE measurements. A conceptional drawing of the equilibrium cell in configuration with the Raman probe is given in Fig. 2.

The setup is capable of operating across a wide range of experimental conditions, with a pressure range from 0.2 kPa to 400 kPa and a temperature range from 278.15 K to 338.15 K, limited by the temperature compensated range of the installed pressure sensor. This flexibility

makes the system suitable for a variety of VLE measurements, allowing for precise characterization of phase equilibria over different temperature and pressure conditions.

3.2. Optical measuring system

The optical measuring system consists of three main components. A fiber-coupled Raman probe, a high throughput spectrometer ((Fig. 1b), and a laser source (Fig. 1a)). The laser and spectrometer are benchtop devices and the Raman probe can be used flexibly due to its fiber coupling. The beam path of the Raman probe is shown in Fig. 3. The laser source is a 532 nm Nd-YAG laser (Genesis CX532–2000 SLM, Coherent), coupled into a fiber (Optran WF 50, NA=0.22, CeramOptek). Inside the Raman probe, an aspherical lens L1 (AL1225 M, Thorlabs GmbH) collimates the laser light, which then passes through a cleaning filter F1 (MaxLine 532/2 (D = 25 mm), Semrock). The filter removes unwanted signals caused by scattering effects that occur as the laser light propagates through the optical fiber. A 45-degree dichroic mirror F2 (RT532rdc, Chroma Technology Corp.) reflects the laser light toward a parabolic mirror (MDP149-P01, Thorlabs GmbH) focusing the laser light into the sample volume. The back scattered light resulting from the Raman effect inside the sample is collected by the parabolic mirror and thus returns through the same beam path. The dichroic mirror F2 reflects the elastically scattered light, and lets the Raman signal pass through.

The Raman light is further filtered by a zero-degree notch filter F3 (532 nm StopLine, Semrock), removing excess laser light, and then focused by an achromatic lens L2 (18 mm Dia. x 22.5 mm FL, VIS-NIR Coated, Achromatic Lens, Edmund Optics) into a fiber (Optran WFGe 50, NA=0.37+/−0.2 CeramOptek), which directs the cleaned-up Raman signal to a high-throughput spectrometer (RAMAN 532 EXR, Wasatch Photonics).

A key feature of the setup is the use of the parabolic mirror, which offers several advantages. By preventing the laser light from passing through a glass lens on the excitation side (after the clean-up filter) of the Raman probe, the disadvantage that glass lenses generate a strong Raman signal (silicon dioxide band) in the wavenumber range up to 1200 cm^{-1}, which overlaps with the fingerprint region of the sample to be measured, is eliminated. Preliminary tests with lenses as focusing element showed a superposition of the fingerprint range (500–1400 cm^{-1}) which can affect spectral evaluation leading to higher deviations and uncertainties. A spectrum which shows the lens's signal is provided in the SI. While this overlap is not problematic for liquid-phase measurements, due to the strong Raman signal of the liquid sample, it can obscure the weak signal from the vapor-phase, leading to poor signal-to-noise ratios and, hence, preventing meaningful data collection. The parabolic mirror effectively minimizes these interferences, improving the quality of measurements, especially for weak vapor-phase signals.

4. Workflow: RaceVLE measurement procedure

In this work, vapor pressure curves and complete pTxy datasets are measured to characterize VLE. Particular emphasis is placed on a robust methodology to distinguish this approach from others. The use of Raman spectroscopy requires system calibration for the measurement of vapor- and liquid-phase compositions. The calibration method follows the procedure outlined by Liebergesell et al. [28]. For the vapor-phase, an indirect calibration is performed, i.e. component is individually calibrated using nitrogen as a reference component. For the liquid-phase, a direct calibration is performed for all substances present in the mixture.

Raman spectra are quantitatively evaluated using the Indirect Hard Modeling (IHM) approach [30,31]. The IHM approach has proven to be very suitable for the quantification of multi-component mixtures with strongly overlapping spectral bands [32]. A detailed description of the method can be found in our previous work [33]. The IHM method models the pure substance spectra as a sum of Voigt functions and is also capable of modeling non-idealities such as background signals using various baseline models and evaluating them on a physical basis. The resulting pure substance models form a linear mixture model, which is fitted to the spectrum of the mixture. Non-linear mixing effects, such as peak shifts, are taken into account by releasing related parameters of the Voigt functions. The fit provides the weights w_i of each pure substance i in the mixture spectrum. These weights w_i are proportional to the corresponding mole fractions x_i of component i in the mixture, so that a linear calibration model can be used to calculate the mole fractions x_i using a calibration constant $k_{i,j}$:

$$\frac{w_i}{w_j} = k_{ij}\frac{x_i}{x_j} \text{ for } i = 1, \ldots, n \text{ and } i \neq j$$

Furthermore, the closing condition applies that the sum of all substance proportions must equal 1:

$$\sum_{i=1}^{n} x_i = 1.$$

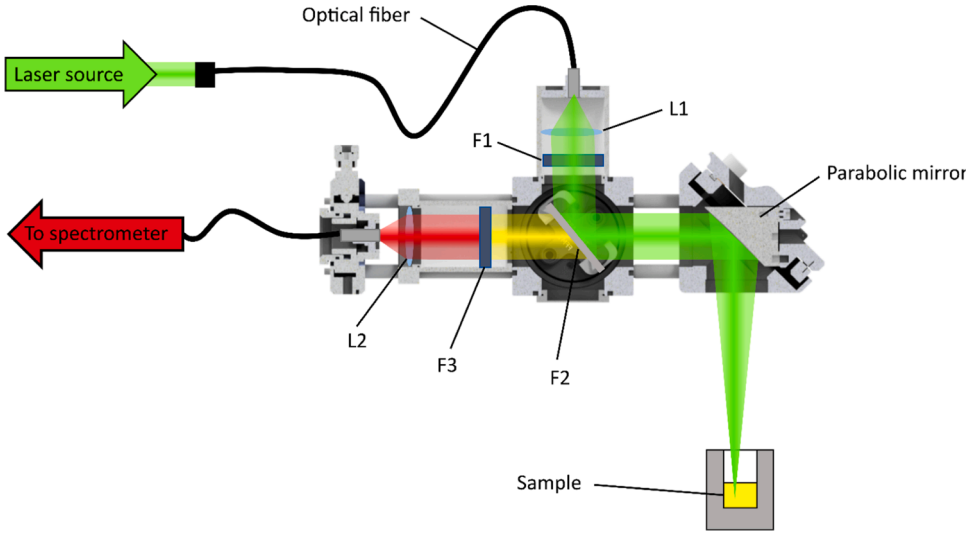

Fig. 3. Beam path of the Raman probe: The laser light from the laser optical fiber is collimated L1 and spectrally corrected F1. A dichroic mirror F2 reflects the light onto a focusing/collecting parabolic mirror. The Raman light from the sample passes through the dichroic mirror F2, is further purified by F3 and focused L2 on the fiber to the spectrometer.

In this section, x_i was assumed to be a generic molar composition for clarity. In the following, x_i is used for the molar composition of the liquid-phase, which follows the same ratiometric IHM principle as described. In 4.2 the same ratiometric IHM calibration principle is used for the vapor-phase with its molar composition y_i.

4.1. Pure-component investigation

In order to be able to use the IHM approach for a quantitative description, pure substance spectra and calibration constants are required, as described above. The calibration constants for the indirect calibration (described in 4.2) are obtained by pressuring a pure substance sample with nitrogen. The composition of the vapor-phase and thus the corresponding calibration constant can then be determined based on the vapor pressure of the pure substance component to be examined and the absolute pressure. It follows that the vapor pressure must be known for each temperature level to be investigated in order to calibrate the system.

For the vapor pressure measurements and pure-component Raman spectra acquisition, the procedure is as follows. The equilibrium cell is tempered to an initial temperature (in this work to 283.15 K). Once the target temperature has been reached, the equilibrium cell is filled with the liquid pure substance. After the liquid is introduced, *in-situ* degassing is performed by opening the valve to vacuum for a short time (approx. 2 s). By evaporation caused by the lowered pressure, the headspace of the sample chamber fills with a vapor-phase and equilibrium is established. The vapor-phase consisting of the pure substance sample and the gases previously dissolved in the sample. With every degassing cycle the pressure lowers until vapor pressure of the pure-component is reached. Degassing cycles are repeated until pressure remains constant after two consecutive degassing steps, it is assumed that the liquid has been sufficiently degassed.

After degassing, a 10-minute waiting period is inserted to allow the system to reach the pure-component phase equilibrium. The pressure is then monitored for a further 5 min to ensure that the fluctuations remain within the specified measurement tolerances of the equipment (0.2 kPa, $0.15 \pm 0.002 * |t|$ in [°C]). If this criterion is satisfied, the system is considered to be in equilibrium and Raman measurements, with the settings described in Section 4.3 are acquired.

In parallel to the vapor pressures which are required for the determination of the calibration constants, pure substance spectra are required for modeling in IHM. These can efficiently be acquired for each temperature level to be investigated during the measurement of the vapor pressures. These steps are repeated for every substance of investigation, one at a time.

To ensure accuracy, the vapor pressure measured of the pure-components can be compared to known pure-component vapor pressures from the literature, if available. This comparison is used to ensure that the system behaves as expected and that the measurements are reliable.

4.2. Vapor-phase calibration

The composition of the vapor-phase, denoted as y, is determined from the Raman signal of the vapor. To calculate the unknown composition of a multicomponent mixture in the vapor-phase, a set of calibration constants $k_{i,vap}$ must be established for each component i.

This calibration is achieved by collecting Raman spectra from mixtures with known compositions. A direct calibration approach would require vapor mixtures of known composition for all investigated substances. However, this direct method is challenging for vapor-phase mixtures as it requires careful preparation of mixtures with well-defined compositions to ensure that no partial condensation occurs that could change the vapor composition. Partial condensation is a major issue in direct calibration, as it changes the vapor mixture. Additionally, in a direct calibration, the mixture must be introduced into a fully evacuated equilibrium cell, making this process difficult to execute reliably for multiple components.

To overcome these challenges, an indirect calibration method is used, as proposed by Liebergesell et al. [29], where nitrogen as non-condensable gas, is introduced beside each investigated pure-component as a reference component. Nitrogen is highly suitable as a reference component due to its specific properties. Nitrogen molecules are chemically inert and exhibit low solubility under the moderate conditions considered in this work. In addition nitrogen molecules generate a Raman signal, which is critical for detection, and their molecular size is sufficient to prevent penetration through the sealing material, ensuring system integrity. In this approach, individual mixtures of each substance and nitrogen are prepared with known compositions, which are calculated based on ideal gas behavior, by pressuring the system with nitrogen. The Raman spectra of these binary mixtures are then used to determine calibration constants $k_{i,N2,vap}$ for each component i in combination with nitrogen as reference component.

$$\frac{w_i}{w_{N_2}} = k_{i,N_2,vap}\frac{y_i}{y_{N_2}} \text{ for } i = 1, \ldots, n$$

From these constants, the desired calibration constants for the multicomponent vapor-phase, $k_{i,j,vap}$ can be derived, allowing the unknown composition of the vapor-phase mixture to be determined from its Raman signal.

$$\frac{w_i}{w_j} = k_{i,j,vap}\frac{y_i}{y_j} \text{ with } k_{i,j,vap} = \frac{k_{i,N_2,vap}}{k_{j,N_2,vap}}$$

Pure-component investigation delivers vapor pressures and pure-component spectra as described in 4.1. Pure-component hard models are derived as described in Section 4.

In the next step, the indirect calibration is performed. Nitrogen is introduced into the equilibrium cell until a target pressure is reached. Raman spectra of the vapor-phase are then recorded under equilibrium conditions. For the purpose of indirect calibration, it is assumed that the addition of nitrogen does not influence the vapor pressure of the components and that the vapor-phase behaves ideally at low pressures.

To obtain a range of calibration data, the composition of the vapor mixture is varied by gradually increasing the partial pressure of nitrogen in the system, while the partial pressure of the pure substance remains constant at a distinct temperature. According to Dalton's law, the absolute pressure is the sum of the partial pressures of nitrogen and the pure substance vapor pressure. By incrementally introducing nitrogen into the volume, the partial pressure of nitrogen in the system is increased in discrete steps, leading to a change in the absolute pressure, enabling the calculation of the molar composition of the vapor-phase as described above. This absolute pressure is continuously measured during the measurement process. Ten Raman spectra are collected at each pressure level under equilibrium conditions.

4.3. Liquid-phase calibration

To determine the unknown composition of the liquid-phase from its Raman signal, a calibration constant $k_{i,j,liq}$ must be established by direct calibration, measuring spectra from liquid mixtures with known compositions. To minimize sample evaporation and thus deviation in the liquid-phase composition, the equilibrium cell is cooled to 283.15 K. Once the equilibrium cell reaches the desired temperature, the sapphire window is removed, and a prepared liquid mixture of known composition is introduced using a syringe. The window is then reattached to seal the equilibrium cell. After thermal equilibrium is reached, 50 Raman spectra of the liquid-phase are acquired. Following spectral acquisition, the equilibrium cell is cleaned by evacuation using a vacuum pump. The process is repeated by removing the sapphire window, introducing a new sample, sealing the equilibrium cell, waiting for thermal equilibrium, recording the spectrum, and cleaning. In this study, five independent loadings of the equilibrium cell were used for liquid-phase

calibration.

In the present work, acquisition times of 60 s at a laser power of 500 mW were used for the vapor-phase analysis. For the analysis of the liquid-phase, 1 s acquisition at 100 mW laser power were used. The significant differences in acquisition time and laser power compared to the vapor-phase measurements are due to the varying densities of the two phases, as the Raman signal is proportional to the number of molecules within the measurement volume. The acquisition times can vary depending on the material system and should therefore be adapted to the substances to be analyzed.

In this work 10 spectra were acquired for investigation of the vapor-phase and 50 for the liquid-phase. To further improve the signal-to-noise ratio, two spectra were summed, resulting in 25 data points for the measurement of the liquid-phase and 5 data points for the vapor-phase per equilibrium. Two representative spectra are shown below in Figs. 4 and 5. The spectra are normalized. The liquid-phase spectrum in Fig. 4 is unprocessed. The vapor-phase spectrum in Fig. 5 is additionally spline corrected. It can be seen that by using lensless focusing, as described in Section 3.2, the fingerprint area of the Raman spectrum is accessible without overexposure due to the strong signal from the glass lenses. Furthermore, the signal of the sapphire band, which is generated by sapphire window of the equilibrium cell, is clearly recognizable in the vapor-phase with three sharp peaks in the wavenumber area between 400 cm^{-1} and 800 cm^{-1}. Overall, the signal to noise ratio is excellent, ensuring reliable and accurate calibration.

4.4. Phase equilibria analysis

In the present work, two types of phase equilibrium measurements were performed, the determination of vapor pressure and binary VLE measurements.

For the measurement of multicomponent VLE data, the equilibrium cell is filled with a pre-weighed sample of 2–3 mL. After filling, the sample is degassed by applying vacuum, as described in Section 4.1 and the system must reach equilibrium, therefore a waiting time is applied, which usually takes 5 to 10 min. Once equilibrium is reached, the stirrer is turned off. The stirring flea is positioned under the steel sleeve. The Raman probe is positioned at the appropriate location using a linear actuator and compositions of the vapor- and liquid-phases are measured. For spectral acquisition in phase analysis, the same exposure times and laser power are used for the vapor- and liquid-phases as for the calibrations described in chapters 4.2 and 4.3. As described for calibration, two spectra are summed to obtain a better signal-to-noise ratio.

After the spectra have been acquired, the valve to vacuum is opened so that the pressure is lowered and part of the sample can evaporate. As the more volatile components are selectively distilled off during this continuous pumping process, the composition of the sample in the equilibrium cell changes. After a short period of pumping, around five to ten seconds, depending on the volatility of the sample, the equilibrium cell is closed again via the membrane valve and a new equilibrium is established at a slightly lower pressure. This step can be repeated until a desired pressure change has been reached. The compositions of the vapor- and the liquid-phase at this new equilibrium are then measured using the same above presented procedure. The process can be repeated until there is no more sufficient liquid-phase in the equilibrium cell for Raman quantification. Depending on the concentration differences between the measurements, 3 to 5 data points per 3 mL sample are usually determined. As soon as the sample is completely distilled and there is no sufficient liquid-phase left, the next prepared sample is introduced, and the process is repeated.

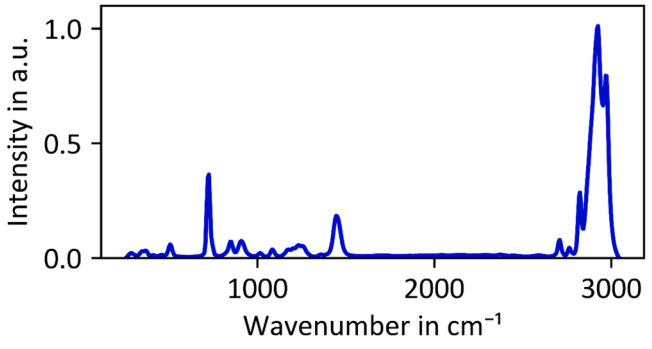

Fig. 4. Normalized liquid-phase spectrum of experiment VLE7 (see Table 3), acquisition time 1 second and 100 mW laser power.

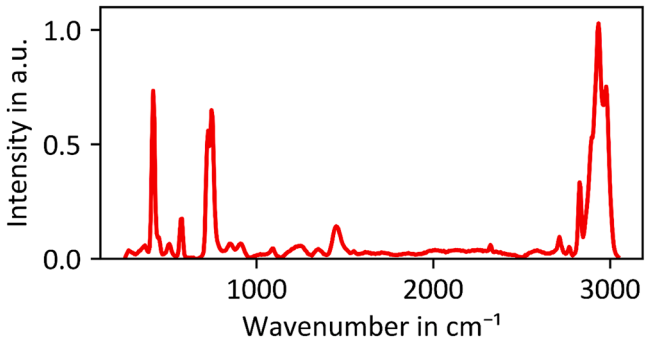

Fig. 5. Normalized vapor-phase spectrum of experiment VLE7 (see Table 3), spline corrected, acquisition time 60 s and 500 mW laser power.

4.5. Materials for validation

To validate the RaceVLE setup, the vapor pressure curves of methyl tert-butyl ether (MTBE), and isooctane, and cyclohexane, were measured. Besides vapor pressure measurements the binary system isooctane-MTBE is measured. The experiments utilized isooctane, MTBE as well as cyclohexane of Uvasol grade, obtained from Merck Millipore (Germany), and nitrogen supplied by Westfalengas (Germany) as shown in Table 1. No additional purification was applied to any of the chemicals, and they were used as provided.

5. Results and discussion

With the introduced setup two pure-component vapor pressure curves and the VLE of isooctane – MTBE are successfully determined. The pure-component vapor pressure measurements were carried out in a range of 283.15 K to 333.15 K. For each temperature level, 60 vapor pressure values were recorded and averaged. Results of our vapor pressure measurements are given in Table 2. Fig. 6 compares our measured vapor pressures with vapor pressure curves calculated using the Antoine equation. The parameters for the Antoine equation calculated vapor pressures are from [34] for MTBE, [35] for isooctane and [36] for cyclohexane.

As shown in Fig. 6 the deviations compared to literature data are very small and therefore excellent agreement with literature data is achieved. The mean measurement uncertainty is $u(p_{s,0}) = 0.02619$ kPa, and hence smaller than the absolute error band of the pressure sensor

Table 1
Used chemicals.

	Cas Number	*Supplier*	*Description*	*purity (GC, A %)*
Iso-octane	540–84–1	Merck Millipore	Uvasol	≥99.8
Methyl tert-butyl ether	1634–04–4	Merck Millipore	Uvasol	≥99.8
Cyclohexane	110–82–7	Merck Millipore	Uvasol	≥99.8
Nitrogen	7727–37–9	Westfalengas	–	>99.999

Table 2
Vapor pressures of isooctane, MTBE and cyclohexane.

Iso-octane		MTBE		Cyclohexane	
T/K	p/kPa	T/K	p/kPa	T/K	p/kPa
283.91	3.45			283.47	7.169
288.04	4.51	288.12	21.81	287.55	8.858
293.07	5.12	293.14	27.34	293.16	11.054
298.13	6.66	298.17	33.86	297.01	13.034
303.17	8.41	303.18	41.43	303.21	17.072
308.37	10.64	308.22	50.48	307.68	20.662
313.2	12.82	313.37	61.23	313.11	25.453
318.25	16.28	318.27	72.96	318.34	31.218
323.22	19.93	323.24	86.94	322.72	36.985
328.45	24.38	328.39	103.1	323.39	37.846
333.11	28.95	333.09	120.12	328.44	45.238
				333.23	53.348

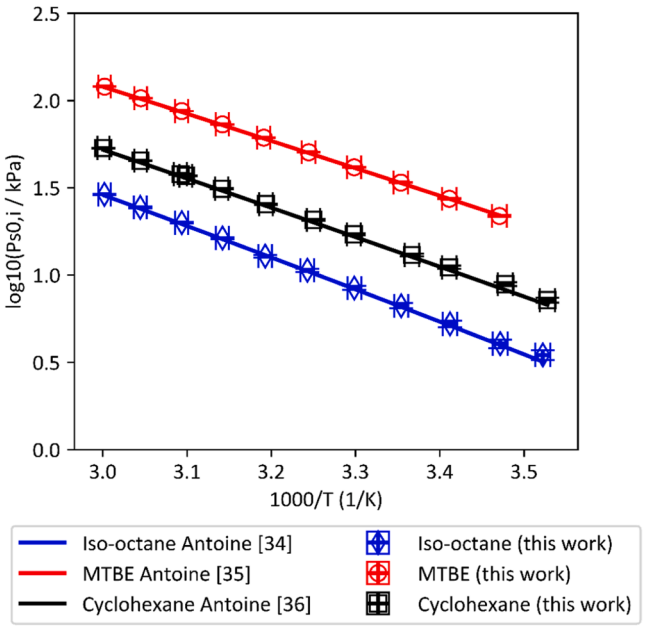

Fig. 6. Vapor pressure curve of isooctane, MTBE and cyclohexane and vapor pressure curve from literature [34–36].

used (0.2 kPa), indicating high measurement precision for the vapor pressure measurements.

5.1. VLE of the binary system MTBE – iso-octane

With the introduced setup, fourteen equilibrium data points for vapor- and liquid-phase were successfully measured. By recording separate spectra, it was possible to check if the system reached the equilibrium state. For new and unknown substances, this can be a great advantage to check whether the system has truly reached equilibrium. A continuous acquiring of the spectra would be conceivable. Fig. 7 shows the variation of mass fractions over 10 min for the vapor-phase and over 50 s for the liquid-phase.

As shown in Fig. 7 deviations in composition over measurement time are very small. This indicates that the chosen equilibration time was sufficient for accurate VLE determination. All VLE data points and standard uncertainties are listed in Table 3. The calibration data, including linear regression models for MTBE and isooctane for both, the vapor- and liquid-phases, are also included in the SI.

For the VLE experiments, the uncertainties were estimated by calculating the standard deviations for molar composition for each equilibrium point. Equilibrium criteria defined in Chapter 4.1 was

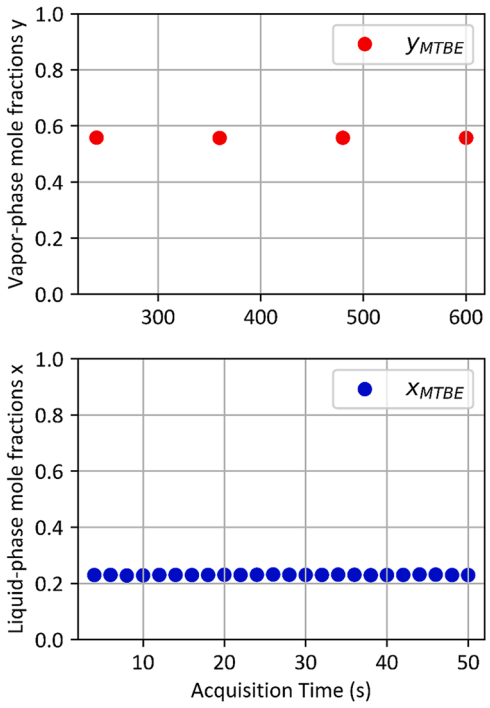

Fig. 7. Molar fractions x,y of MTBE over time after equilibration as described in Section 4.1 and start of the first acquisition (VLE 4 in Table 3).

Table 3
Isothermal vapor-liquid equilibrium mole fractions for the system MTBE and isooctane at $T = 318.15$ K.

	Pressure in kPa	x_{MTBE}	y_{MTBE}	u(x_{MTBE})	u(y_{MTBE})
VLE 1	18.984	0.081	0.223	0.002	0.003
VLE 2	20.318	0.098	0.279	0.001	0.004
VLE 3	28.087	0.208	0.508	0.001	0.005
VLE 4	30.020	0.230	0.558	0.001	0.001
VLE 5	31.329	0.245	0.570	0.001	0.004
VLE 6	40.985	0.411	0.760	0.001	0.001
VLE 7	41.761	0.420	0.761	0.001	0.006
VLE 8	42.353	0.423	0.766	0.001	0.005
VLE 9	50.068	0.586	0.853	0.002	0.001
VLE 10	55.459	0.696	0.893	0.002	0.001
VLE 11	55.630	0.690	0.899	0.004	0.005
VLE 12	56.437	0.711	0.900	0.003	0.002
VLE 13	56.649	0.716	0.894	0.002	0.003
VLE 14	66.320	0.891	0.961	0.001	0.004

applied to ensure that the standard deviations shown in Table 3 represent fully equilibrated systems. These uncertainties reflect the variance in the measurements and provide information about the precision of the setup. The standard uncertainties, u(x_{MTBE}) and u(y_{MTBE}) for each equilibrium point for the VLE MTBE and isooctane are given in Table 3.

Fig. 8 compares the data from Table 3 with the measurements of Bernatová et al. at 318.15 K, as shown in a pTxy diagram [37]. The agreement between the equilibrium mole fractions for both the saturated liquid and vapor lines is excellent, especially when considering the mean uncertainties for the liquid-phase measurements u(x_{MTBE})= 0.0016 and for the vapor-phase measurements u(y_{MTBE})=0.0033, which confirms the high precision of the setup.

These results demonstrate the overall reliability and reproducibility of the phase equilibrium measurements. With the presented setup it was possible to measure the full VLE (14 VLE equilibrium compositions) in 5 h consuming <42 mL of sample volume overall.

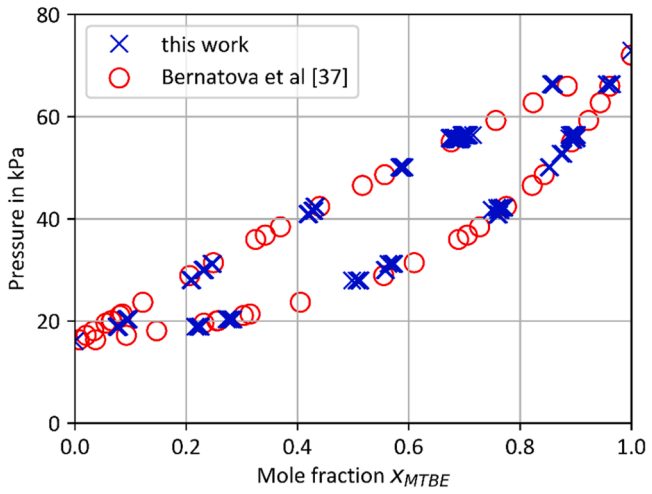

Fig. 8. VLE MBTE-Iso-Octane measured at 318.15 K with the presented setup and data from Bernatová et al. [37].

6. Conclusion and outlook

This work presents, an innovative and highly efficient setup for the determination of isothermal vapor-liquid equilibria (VLE) using Raman spectroscopy. Very accurate and, fast *in-situ* VLE determination, for a wide range of temperature and pressure conditions, with very low sample consumption combined with special emphasis on ease of use.

The setup is centered around a compact and robust measurement system and a user-friendly equilibrium cell requiring a small sample volume. The small dimensions of the sample chamber enable efficient measurements of vapor pressure curves and multicomponent VLE. *In-situ* concentration measurements via Raman spectroscopy are precise and time-saving, reducing experimental effort and avoiding errors associated with manual sampling and *ex-situ* analysis.

Calibration procedure is designed to minimize effort and sample consumption. Indirect vapor-phase calibration requires only 2 mL per component and calibration and is reusable for each component, since it is calibrated against nitrogen. Liquid-phase calibration requires approximately 10 mL per system. Full calibration is completed within approx. 4 h, including cleaning and safety buffers.

Each equilibrium point, consisting of vapor- and liquid-phase measurements can be measured in just 20 min, and the complete VLE (14 equilibrium points) was measured within 5 h consuming <42 mL of chemicals.

Future work will focus on the measurement of multicomponent (ternary and higher dimension) VLE and the automation of the measurement setup and subsequent data analysis. This efficient methodology will help accelerate research on newly synthesized substances that are often only available in limited quantities. By enabling precise VLE measurements of such materials, it will not only improve the reliability and speed of classical process design, but also support the seamless upscaling of processes with novel compounds.

CRediT authorship contribution statement

Marvin Kasterke: Writing – original draft, Visualization, Validation, Software, Project administration, Methodology, Investigation, Formal analysis, Data curation, Conceptualization. **Leo Bahr:** Writing – review & editing, Supervision, Funding acquisition, Conceptualization. **Hans-Jürgen Koß:** Writing – review & editing, Supervision, Resources, Funding acquisition, Conceptualization. **Thorsten Brands:** Writing – review & editing, Supervision, Resources, Conceptualization.

Declaration of competing interest

The authors declare the following financial interests/personal relationships which may be considered as potential competing interests:

Marvin Kasterke reports financial support was provided by German Research Foundation. If there are other authors, they declare that they have no known competing financial interests or personal relationships that could have appeared to influence the work reported in this paper.

Acknowledgements

This work was funded the Deutsche Forschungsgemeinschaft (DFG, German Research Foundation) – 471272247

Supplementary materials

Supplementary material associated with this article can be found, in the online version, at doi:10.1016/j.fluid.2025.114344.

Data availability

Data will be made available on request.

References

[1] E. Hendriks, G.M. Kontogeorgis, Industrial requirements for thermodynamics and transport properties, Ind. Eng. Chem. Res. 49 (22) (2010) 11131–11141.
[2] P. Uusi-Kyyny. Vapour Liquid Equilibrium Measurements For Process Design, Helsinki University of Technology, 2004, 951-22-7364-0, https://www.researchgate.net/publication/27516297_Vapour_Liquid_Equilibrium_Measurements_for_Process_Design.
[3] I.C. Arango, A.L. Villa, Isothermal vapor-liquid and vapor-liquid-liquid equilibrium for the ternary system ethanol+ water+ diethyl carbonate and constituent binary systems at different temperatures, Fluid Phase Equilib. 339 (2013) 31–39.
[4] Materials for Separation Technologies. Energy and Emission Reduction Opportunities, Oak Ridge National Laboratory (ORNL), Oak Ridge, TN, United States, 2005. https://doi.org/10.2172/1218755.
[5] J.L. Humphrey, G.E. Keller, Separation Process Technology, McGraw-Hill, New York, 1997.
[6] T. Holderbaum, J. Gmehling, PSRK: a group contribution equation of state based on UNIFAC, Fluid Phase Equilib. 70 (2–3) (1991) 251–265.
[7] M.L. Corazza, W.A. Fouad, W.G. Chapman, PC-SAFT predictions of VLE and LLE of systems related to biodiesel production, Fluid Phase Equilib. 416 (2016) 130–137, https://doi.org/10.1016/j.fluid.2015.09.044.
[8] R. Wittig, J. Lohmann, J. Gmehling, Vapor−Liquid Equilibria by UNIFAC group contribution. 6. Revision and extension, Ind. Eng. Chem. Res. 42 (1) (2003) 183–188, https://doi.org/10.1021/ie020506l.
[9] A. Klamt, COSMO-RS: From quantum Chemistry to Fluid Phase Thermodynamics and Drug Design, 1st ed., Elsevier, Amsterdam, 2005.
[10] A.L. Muhlbauer, J.D. Raal, Phase Equilibria: measurement & Computation (1st ed.), 1997 https://doi.org/10.1201/9780203743621.
[11] G.M. Kontogeorgis, G.K. Folas, Thermodynamic Models For Industrial applications: from Classical and Advanced Mixing Rules to Association Theories, John Wiley & Sons, 2009.
[12] R. Dohrn, J.M.S. Fonseca, S. Peper, Experimental methods for phase equilibria at high pressures (in eng), Annu. Rev. Chem. Biomol. Eng. 3 (2012) 343–367, https://doi.org/10.1146/annurev-chembioeng-062011-081008.
[13] S.K. Luther, J.J. Schuster, A. Leipertz, A. Braeuer, Non-invasive quantification of phase equilibria of ternary mixtures composed of carbon dioxide, organic solvent and water, J. Supercrit. Fluids 84 (2013) 146–154, https://doi.org/10.1016/j.supflu.2013.09.012.
[14] Y. Leusmann, M.G. Hopkins, E.F. May, P.L. Stanwix, M. Richter, Framework for in situ measurements of vapor–liquid equilibrium using a microwave cavity resonator, Int. J. Thermophys. 44 (1) (2023), https://doi.org/10.1007/s10765-022-03098-7.
[15] J.D. Raal, D. Ramjugernath, 5 Vapour—Liquid equilibrium at low pressure, in: R.D. Weir, TH.W. De Loos (Eds.), Measurement of the Thermodynamic Properties of Multiple Phases, Experimental Thermodynamics, 7, pp. 71–87. https://doi.org/10.1016/S1874-5644(05)80007-4.
[16] S. Peper, R. Dohrn, Sampling from fluid mixtures under high pressure: review, case study and evaluation, J. Supercrit. Fluids 66 (2012) 2–15, https://doi.org/10.1016/j.supflu.2011.09.021.
[17] C.E. Schwarz, Preface to nontraditional techniques for measurement of phase equilibria special issue, J. Chem. Eng. Data 65 (7) (2020) 3261, https://doi.org/10.1021/acs.jced.0c00547.
[18] M.H.H. Fechter, A.S. Braeuer, Vapor-Liquid Equilibria of Mixtures Containing Ethanol, Oxygen, and Nitrogen at Elevated Pressure and Temperature, Measured

with In Situ Raman Spectroscopy in Microcapillaries (in eng), J. Chem. Eng. Data 65 (7) (2020) 3373–3383, https://doi.org/10.1021/acs.jced.0c00184.
[19] A. Gomis, J. García-Cano, A. Font, M.D. Saquete, J.C. Asensi, V. Gomis, Use of ultrasound in the determination of isobaric LLV, SLV, and SLLV equilibrium data. application to the determination of the water + Na 2 SO 4 or K 2 SO 4 + 2-Methylpropan-2-ol Systems at 101.3 kPa and Boiling Conditions, J. Chem. Eng. Data 65 (7) (2020) 3287–3296, https://doi.org/10.1021/acs.jced.0c00065.
[20] C.L. Suiter, V.D. Malavé, E.J. Garboczi, J.A. Widegren, M.O. McLinden, Nuclear magnetic resonance (NMR) spectroscopy for the in situ measurement of vapor–liquid equilibria, J. Chem. Eng. Data 65 (7) (2020) 3318–3333, https://doi.org/10.1021/acs.jced.0c00113.
[21] M.A. Khoshooei, D. Sharp, Y. Maham, A. Afacan, G.P. Dechaine, A new analysis method for improving collection of vapor-liquid equilibrium (VLE) data of binary mixtures using differential scanning calorimetry (DSC), Thermochim. Acta 659 (2018) 232–241, https://doi.org/10.1016/j.tca.2017.12.010.
[22] T. Kaiser, C. Voßmerbäumer, G. Schweiger, A new approach to the determination of fluid phase Equilibria: concentration measurements by Raman spectroscopy, Ber. Bunsenges. Phys. Chem. 96 (8) (1992) 976–980, https://doi.org/10.1002/bbpc.19920960805.
[23] R. Adami, J. Schuster, S. Liparoti, E. Reverchon, A. Leipertz, A. Braeuer, A Raman spectroscopic method for the determination of high pressure vapour liquid equilibria, Fluid Phase Equilib. 360 (2013) 265–273, https://doi.org/10.1016/j.fluid.2013.09.046.
[24] A. Stratmann, G. Schweiger, Fluid phase equilibria of ethanol and carbon dioxide mixtures with concentration measurements by raman spectroscopy, Appl. Spectrosc. 56 (6) (2002) 783–788, https://doi.org/10.1366/000370202760077531.
[25] S.K. Luther, S. Stehle, K. Weihs, S. Will, A. Braeuer, Determination of vapor-liquid equilibrium data in microfluidic segmented flows at elevated pressures using Raman spectroscopy (in eng), Anal. Chem. 87 (16) (2015) 8165–8172, https://doi.org/10.1021/acs.analchem.5b00699.
[26] T.C. Klima, A.S. Braeuer, Vapor-liquid-equilibria of fuel-nitrogen systems at engine-like conditions measured with Raman spectroscopy in micro capillaries, Fuel 238 (2019) 312–319, https://doi.org/10.1016/j.fuel.2018.10.108.
[27] M.H. Fechter, J. Koschack, A.S. Braeuer, Vapor-Liquid equilibria of the systems 1-octanol/nitrogen and 1-octanol/oxygen at pressures from 3 to 9 MPa and temperatures up to 613 K – Measured in a microcapillary with Raman spectroscopy, Fuel 323 (2022) 124352, https://doi.org/10.1016/j.fuel.2022.124352.
[28] B. Liebergesell, C. Flake, T. Brands, H.-J. Koß, A. Bardow, A milliliter-scale setup for the efficient characterization of isothermal vapor-liquid equilibria using Raman spectroscopy, Fluid Phase Equilib. 446 (2017) 36–45, https://doi.org/10.1016/j.fluid.2017.04.014.
[29] B. Liebergesell, T. Brands, H.-J. Koß, A. Bardow, Quaternary isothermal vapor-liquid equilibrium of the model biofuel 2-butanone + n-heptane + tetrahydrofuran + cyclohexane using Raman spectroscopic characterization, Fluid Phase Equilib. 472 (2018) 107–116, https://doi.org/10.1016/j.fluid.2018.04.009.
[30] F. Alsmeyer, H.J. Koß, W. Marquardt, Indirect spectral hard modeling for the analysis of reactive and interacting mixtures, Appl. Spectrosc. 58 (8) (2004) 975–985, https://doi.org/10.1366/0003702041655368.
[31] P. Beumers, D. Engel, T. Brands, H.-J. Koß, A. Bardow, Robust analysis of spectra with strong background signals by First-Derivative Indirect Hard Modeling (FD-IHM), Chemom. Intell. Lab. Syst. 172 (2018) 1–9, https://doi.org/10.1016/j.chemolab.2017.11.005.
[32] C. Peters, et al., Multicomponent diffusion coefficients from microfluidics using Raman microspectroscopy (in eng), Lab Chip 17 (16) (2017) 2768–2776, https://doi.org/10.1039/c7lc00433h.
[33] J. Thien, L. Reinpold, T. Brands, H.-J. Koß, A. Bardow, Automated physical property measurements from calibration to data analysis: microfluidic platform for liquid–liquid equilibrium using raman microspectroscopy, J. Chem. Eng. Data 65 (2) (2020) 319–327, https://doi.org/10.1021/acs.jced.9b00636.
[34] T. Boublik, V. Fried, E. Hala, The Vapour Pressures of Pure Substances, Elsevier Science Pub. Co., Inc., New York, NY, United States, 1984 [Online]. Available: https://www.osti.gov/biblio/6997933.
[35] S. Horstmann, H. Gardeler, R. Bölts, D. Zudkevitch, J. Gmehling, Vapor−liquid equilibria and excess enthalpy data for the binary systems 2-methyltetrahydrofuran with 2,2,4-Trimethylpentane (Isooctane), ethanol, toluene, cyclohexane, and methylcyclohexane, J. Chem. Eng. Data 44 (5) (1999) 959–964, https://doi.org/10.1021/je990023x.
[36] W.J. Kerns, R.G. Anthony, P.T. Eubank, Volumetric Properties of Cyclohexane Vapor, AIChE Symp. Ser. 70 (140) (1974) 14–21.
[37] S. Bernatová, I. Wichterle, Isothermal vapour–liquid equilibria in the ternary system tert-butyl methyl ether + tert-butanol + 2,2,4-trimethylpentane and the three binary subsystems, Fluid Phase Equilib. 180 (1–2) (2001) 235–245, https://doi.org/10.1016/S0378-3812(01)00349-1.